Mesonic excitations of QGP: Study with an effective model

Paramita Deb[*] and Abhijit Bhattacharyya[†]
Department of Physics, University of Calcutta, 92, A. P. C. Road, Kolkata-700009, India

Saumen Datta[‡]
Department of Theoretical Physics, Tata Institute of Fundamental Research, Homi Bhabha Road, Mumbai-400005, India

Sanjay K. Ghosh[§]
Centre for Astroparticle Physics & Space Science and Department of Physics, Bose Institute, 93/1, A. P. C Road, Kolkata-700009, India
(Received 15 January 2009; published 28 May 2009)

We study the correlations between quark-antiquark pairs in different quantum number channels in a deconfined plasma by using an effective model of QCD. Using the three flavor PNJL model, the finite temperature spectral functions for different mesonic states are studied at zero and nonzero quark chemical potentials. It is found that in the η channel, resonance structures survive above the chiral transition temperature T_χ, while the kaonic states seem to get washed off just above T_χ. The sensitivity of the structures to the anomaly term are carefully investigated.

DOI: 10.1103/PhysRevC.79.055208 PACS number(s): 25.75.Nq, 12.38.Mh, 11.30.Rd, 12.39.−x

I. INTRODUCTION

At high temperatures and densities, strongly interacting matter is expected to undergo a transition to new phases where color degrees of freedom are deconfined. Such conditions of high temperatures and densities can be created in the laboratory by the collision of heavy ions at large energies. A large amount of data has already been obtained from the BNL Relativistic Heavy Ion Collider (RHIC). In the near future, results will be available from the CERN Large Hadron Collider (LHC) for the low density and high temperature phase. On the other hand, the experiment at the GSI Facility for Antiproton and Ion Research (FAIR) will provide us information about extremely dense matter at low temperature. It is thus extremely relevant to study the properties of strongly interacting matter at high temperature and density.

A first-principle study of hot and dense strongly interacting matter starting from QCD is not easy because the physics is nonperturbative in the temperature and density range of interest. At finite temperatures, numerical studies on the lattice provide the most reliable results for the physics of the deconfined phase. The physics of excitations in real time, however, is not directly accessible from the lattice, and one requires an analytical continuation from Euclidean time. Studies at finite baryon number density are prohibitively difficult on the lattice because of the well-known sign problem. Some progress has been made in recent years in extracting results for small densities [1,2]. As it stands now, the lattice predicts that deconfinement and chiral symmetry restoration happen roughly simultaneously [3] via a smooth crossover [4] at zero quark chemical potential, and the two transitions roughly coincide at about $T_\chi \sim 180$–200 MeV [3]. There is an indication of a critical point at a small chemical potential $\mu_B \approx 300$–500 MeV, with a first-order transition for larger μ_B [1]. There have also been suggestions that the first-order line may not exist [2].

In view of the limitations in studying finite density and real time problems, it may be useful to get an idea of the features of the new phases of matter by studying QCD-inspired models. Depending on the physics of interest, one can attempt to study a model that has features relevant to the physics issue. In particular, for issues of the transition of the hadronic matter to a chiral-symmetry-restored deconfined phase, the Polyakov loop extended Nambu–Jona-Lasinio (PNJL) model has been used.

In the Nambu–Jona-Lasinio (NJL) model [5,6], as it is used currently, the interactions between quarks are taken into account by suitable four-quark terms that respect the chiral symmetry of the QCD Lagrangian. Since the gluons are integrated out, with their only effect being the four-quark interaction terms, there is no confinement *per se* in this model. The chiral symmetry is, however, spontaneously broken by $\bar{q}q$ condensation: $U_L(N_f) \times U_R(N_f) \to U_V(N_f)$. As a result, the quarks pick up a constituent mass. Furthermore, the pseudoscalar mesons π, K, and η become the Goldstone modes. It is also easy to incorporate the $U_A(1)$ anomaly by introducing a suitable determinant term [6]. The NJL model has been widely used to study the chiral phase transition in QCD and the nature of the excitations at temperatures slightly above the transition temperatures. Based on such studies, it was suggested sometime back that nontrivial strong correlations between $q\bar{q}$ pairs persist in the deconfined phase at moderately high temperatures [6].

Because of the lack of confinement, though, the NJL model does miss out on some important aspects of the QCD thermal transition. In particular, the chiral transition in QCD is also of a deconfining nature, as the Polyakov loop, which is the confinement-deconfinement order parameter, shows a rapid change. The Polyakov loop extended NJL (PNJL) model [7]

[*]paramita.deb83@gmail.com
[†]abphy@caluniv.ac.in
[‡]saumen@theory.tifr.res.in
[§]sanjay@bosemain.boseinst.ac.in

 ©2009 The American Physical Society

attempts to capture this feature of the QCD transition. In this model, the gluon dynamics is described by a background temporal gluon field which is coupled to the quarks by the covariant derivative. The value of the background field is determined by minimizing the corresponding potential $U(\Phi)$ which depends on the traced Polyakov loop Φ.

The PNJL model has been extensively used to look at the phase structure at high temperature and density. Ratti *et al.* [8] have studied the two flavor version of this model in a certain amount of detail. They have looked at the crossover transition around 200 MeV and the quark number densities at different baryonic chemical potentials. Their results match nicely with the lattice, especially the fact that the chiral restoration and the deconfinement transition take place almost simultaneously. The speed of sound and the diagonal susceptibilities, calculated with the PNJL model, were also found to be in good agreement with lattice results [9]. On the other hand, the off-diagonal susceptibilities in the two flavor PNJL model differ from the lattice results [10]. Recently Fukushima studied the phase diagram of the three flavor quark matter within the framework of the PNJL model [11].

Since the PNJL model successfully reproduces a large number of quantities calculable directly from QCD, one may be interested to use this model to study quantities of experimental interest that cannot be directly studied from lattice. In particular, a knowledge of the nature of excitations of the plasma is phenomenologically very important. The complete in-medium behavior of the mesonic excitations require a study of the spectral functions in these channels. As we discussed earlier, it is not easy to calculate them on the lattice. A detailed study of such spectral functions in the NJL model was carried out sometime back [6]. It is clearly of interest to find out how the introduction of the Polyakov loop changes the nature of the $q\bar{q}$ correlations. Hansen *et al.* [12] have studied the pion and σ correlation functions in the two flavor PNJL model. Costa *et al.* [13] have calculated the masses of the pseudoscalar mesons at finite temperature and zero density. It is, of course, interesting and phenomenologically important to study a larger set of mesonic correlations for the realistic case of the $2+1$ flavor PNJL model and also at finite density.

Here we aim to carry out such a study. We look at the spectral functions and pole masses of the pseudoscalar channels with different flavor contents. We also carefully investigate the effect of the anomaly term in the spectral functions. The spectral functions have also been studied in the presence of a small chemical potential.

In the next section, we briefly describe the $2+1$ flavor PNJL model, as used by us. In Sec. III, the basic in-medium calculations and the chiral transition are discussed. The main results of the paper, about mesonic excitations, are given in Sec. IV. A summary of our results and conclusions are available in the last section.

II. THREE FLAVOR PNJL MODEL

In this section, we briefly describe the PNJL model, and specify the parameters of the model that we have used. More details can be found in the literature [7,8,14].

In the NJL model, the gluon dynamics is reduced to the chiral point couplings between quarks. The PNJL model also introduces the temporal gauge field, since the Polyakov loop

$$\Phi = \frac{1}{V}\int d^3x \frac{1}{N_c}\,\mathrm{Tr}\,\mathcal{P}\exp\left[i\int_0^\beta d\tau A_4(\vec{x},\tau)\right] \tag{1}$$

is the order parameter for the confinement-deconfinement transition. Here $A_4 = iA_0$ is the temporal component of the Euclidean gauge field, $\beta = 1/T$, and $\mathcal{P}$ denotes path ordering. Our effective $\mathrm{SU}(3)_f$ Lagrangian is [14]

$$\begin{aligned}\mathcal{L} &= \sum_{f=u,d,s}\bar{\psi}_f\gamma_\mu i D^\mu\psi_f - \sum_f m_f\bar{\psi}_f\psi_f + \sum_f \mu\gamma_0\bar{\psi}_f\psi_f \\ &\quad + \frac{g_S}{2}\sum_{a=0,\ldots,8}[(\bar{\psi}\lambda^a\psi)^2 + (\bar{\psi}i\gamma_5\lambda^a\psi)^2] \\ &\quad - g_D[\det\bar{\psi}_f(1+\gamma_5)\psi_{f'} + \det\bar{\psi}_f(1-\gamma_5)\psi_{f'}] \\ &\quad - \mathcal{U}(\Phi[A],\bar{\Phi}[A],T) \\ &= \mathcal{L}_0 + \mathcal{L}_\mathcal{M} + \mathcal{L}_\mu + \mathcal{L}_s + \mathcal{L}_{\mathcal{KMT}} - \mathcal{U}.\end{aligned} \tag{2}$$

In the above Lagrangian, $\mathcal{L}_0$ is the kinetic term with gauge field interactions, $D^\mu = \partial^\mu - iA_4\delta_{\mu 4}$. The gauge coupling is absorbed in the definition of A^μ. $\mathcal{L}_M$ is the mass term which breaks the chiral symmetry explicitly. The mass of a particular flavor is denoted by m_f, and the corresponding field is ψ_f. The light quark mass is considered to be $\sim$5 MeV, and the strange quark mass is considered to be $\sim$140 MeV. The term $\mathcal{L}_s$ is responsible for the four-fermion interaction among the quarks with coupling g_s. Here we take this coupling to be positive. The next term $\mathcal{L}_{\mathcal{KMT}}$, which is a six-fermion interaction, is invariant under $\mathrm{SU}(3)_L \times \mathrm{SU}(3)_R$ but breaks $U(1)_A$ symmetry. This term represents the axial anomaly of QCD [6]. Here "det" stands for the determinant with respect to the flavor indices, and the anomalous coupling is represented as g_D. This anomaly term is responsible for the flavor mixing of η_0 and η_8 mesons in the pseudoscalar channel, giving rise to the η and η' mesons. The potential $U(\Phi)$ is expressed in terms of the Polyakov loop Φ and its conjugate $\bar{\Phi}$ as [8]

$$\frac{\mathcal{U}(\Phi,\bar{\Phi},T)}{T^4} = -\frac{b_2(T)}{2}\bar{\Phi}\Phi - \frac{b_3}{6}(\Phi^3+\bar{\Phi}^3) + \frac{b_4}{4}(\bar{\Phi}\Phi)^2, \tag{3}$$

where

$$b_2(T) = a_0 + a_1\left(\frac{T_0}{T}\right) + a_2\left(\frac{T_0}{T}\right)^2 + a_3\left(\frac{T_0}{T}\right)^3, \tag{4}$$

b_3 and b_4 being constants, and T_0, which is a parameter here, is chosen to be 190 MeV.

Both Φ and $\bar{\Phi}$ are treated as classical field variables. When the quark number density is zero, one has $\Phi = \bar{\Phi}$. This quantity can be considered as the order parameter for the phase transition. Furthermore, $U[\Phi,\bar{\Phi},T]$ has a $Z(3)$ center symmetry which encompasses the phase transition in QCD. At low temperature, U has a single minimum at $\Phi = 0$. At high temperature, U has three degenerate minima at $\Phi = 1, e^{\pm 2i\pi/3}$.

To study the chiral transition, we study the system of Eq. (2) in the mean field approximation (MFA) to get the field equations for Φ, $\bar{\Phi}$, and σ. Because of the breaking of

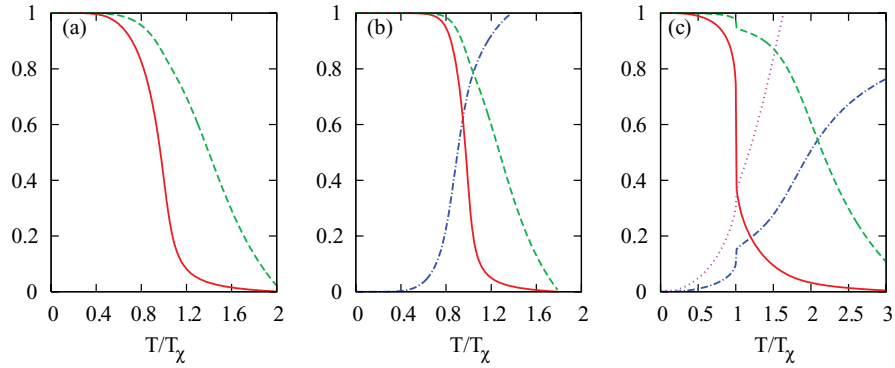

FIG. 1. (Color online) $\langle\bar{u}u\rangle(T)/\langle\bar{u}u\rangle(T=0)$ (red, solid) and $\langle\bar{s}s\rangle(T)/\langle\bar{s}s\rangle(T=0)$ (green, dashed), as a function of T/T_χ at $\mu_q = 0$ for (a) the NJL model and (b) the PNJL model; also shown is the Polyakov loop expectation value, Φ (blue, dash-dotted). (c) Same as (b), but for $\mu_q = 320$ MeV. Here Φ (blue, dash-dotted) and $\bar{\Phi}$ (pink, dotted) are different.

$SU(3)_L \times SU(3)_R$ symmetry to $SU(3)_V$, the quark condensate acquires a nonzero vacuum expectation value given by

$$\langle\bar{\psi}_f\psi_f\rangle = -iN_c\mathcal{L}t_{y\to x^+}(\mathrm{Tr}\,S_f(x-y)), \tag{5}$$

where trace is over color and spin states. Also, eight Goldstone bosons appear for the $N_f = 3$ model. The self-consistent gap equation for the constituent masses are

$$\begin{aligned} M_u &= m_u - 4g_S\sigma_u + 2g_D\sigma_d\sigma_s, \\ M_d &= m_d - 4g_S\sigma_d + 2g_D\sigma_s\sigma_u, \\ M_s &= m_s - 4g_S\sigma_s + 2g_D\sigma_u\sigma_d. \end{aligned} \tag{6}$$

Here $\sigma_f = \langle\bar{\psi}_f\psi_f\rangle$ denotes the chiral condensate of a quark with flavor f, where $f = u, d, s$. The expression for σ_f at $T = 0$ and $\mu = 0$ can be written as [14]

$$\sigma_f = -\frac{3M_f}{\pi^2}\int_0^\Lambda \frac{p^2}{\sqrt{p^2 + {M_f}^2}}\,dp, \tag{7}$$

Λ being the three-momentum cutoff.

The parameters of the NJL part of the Lagrangian are fixed at $T = \mu = 0$. In the present work, we have used the parameter set obtained in Ref. [6]:

$$\begin{aligned} &\Lambda = 631.4\ \text{MeV}, \quad m_u = m_d = 5.5\ \text{MeV}, \\ &m_s = 135.7\ \text{MeV}, \quad g_S\Lambda^2 = 3.67, \quad g_D\Lambda^5 = 9.29. \end{aligned}$$

This parameter set reproduces the physical values of the pion mass, $m_\pi = 138$ MeV; pion decay constant, $f_\pi = 93$ MeV; and masses of the K and η' mesons, $m_K = 495.7$ MeV and $m_{\eta'} = 957.5$ MeV. The parameters of $U(\Phi)$ are [8,14]

$$\begin{aligned} &a_0 = 6.75, \quad a_1 = -1.95, \quad a_2 = 2.625, \quad a_3 = -7.44, \\ &b_3 = 0.75, \quad b_4 = 7.5, \quad T_0 = 190\ \text{MeV}, \end{aligned}$$

so as to reproduce the lattice measurements of the Polyakov loop expectation value.

III. CHIRAL TRANSITION IN PNJL MODEL

In the mean field approximation, the thermodynamic potential of the PNJL model can be written as [14]

$$\begin{aligned} &\Omega(\Phi, \bar{\Phi}, M, T, \mu) \\ &= \mathcal{U}[\Phi, \bar{\Phi}, T] + 2g_S\sum_{f=u,d,s}\sigma_f^2 - 4g_D\sigma_u\sigma_d\sigma_s \\ &\quad - T\sum_n\int\frac{d^3p}{(2\pi)^3}\,\mathrm{Tr}\ln\frac{S^{-1}(i\omega_n, \vec{p})}{T}, \end{aligned} \tag{8}$$

where S^{-1} is the inverse quark propagator

$$S^{-1}(p_0, \vec{p}) = \gamma_0(p^0 + \mu - iA_4) - \vec{\gamma}\cdot\vec{p} - M, \tag{9}$$

and $\omega_n = \pi T(2n+1)$ are the Matsubara frequencies of fermions. Using the identity $\mathrm{Tr}\ln(X) = \ln\det(X)$, and performing the color trace, we get

$$\begin{aligned} \Omega &= \mathcal{U}[\Phi, \bar{\Phi}, T] + 2g_S\sum_{f=u,d,s}\sigma_f^2 - 4g_D\sigma_u\sigma_d\sigma_s \\ &\quad - 6\sum_f\int_0^\Lambda\frac{d^3p}{(2\pi)^3}E_{pf}\Theta(\Lambda - |\vec{p}|) - 2\sum_f T\int_0^\infty\frac{d^3p}{(2\pi)^3} \\ &\quad \times\Big\{\ln\Big[1 + 3\Big(\Phi + \bar{\Phi}e^{-\frac{E_{pf}-\mu}{T}}\Big)e^{-\frac{E_{pf}-\mu}{T}} + e^{-3\frac{E_{pf}-\mu}{T}}\Big] \\ &\quad + \ln\Big[1 + 3\Big(\bar{\Phi} + \Phi e^{-\frac{E_{pf}+\mu}{T}}\Big)e^{-\frac{E_{pf}+\mu}{T}} + e^{-3\frac{E_{pf}+\mu}{T}}\Big]\Big\}, \end{aligned} \tag{10}$$

where $E_{pf} = \sqrt{p^2 + M_f^2}$ is the single-quasiparticle energy. In the above integrals, the vacuum integral has a cutoff Λ, whereas the medium-dependent integrals have been extended to infinity.

To look at thermal behavior of different observables, we need to study the variation with temperature of the minimum of the thermodynamic potential. In Fig. 1, we show the thermal behavior of the chiral condensates for both the light and the strange quarks, in both NJL and PNJL models. The NJL results can be obtained from Eq. (10) by setting $U[\Phi, \bar{\Phi}, T] = 0$, $\Phi = 1$, and $\bar{\Phi} = 1$. Figure 1 shows a rapid drop in $\langle\bar{u}u\rangle$ in both the models in the temperature range 150–200 MeV, without any singularity, indicating a chiral-symmetry-restoring crossover. This is consistent with what lattice studies find for QCD [4]. From the points of inflexion of $\langle\bar{u}u\rangle(T)$, one estimates $T_\chi \sim 170$ MeV for NJL and 190 MeV for PNJL models. Figure 1 also shows the behavior of the Polyakov loop, Φ.[1] We see that the deconfinement temperature $T_d \sim T_\chi$, as expected from lattice studies of QCD [3].

[1] In Fig. 1, the value of the Polyakov loop becomes slightly higher than unity for the temperature above 260–300 MeV. At finite density, the value of $\bar{\Phi}$ can go even to 1.4. This is an important *physical problem* in the simple-minded PNJL model as Φ being the normalized trace of the Wilson line L, which is an SU(3) matrix, should lie in the range $0 \leqslant \Phi \leqslant 1$. The natural way to cure this problem is to consider a proper Jacobian of transformation from the matrix valued field L to the complex valued field Φ, which will then constrain the value of $\Phi < 1$ [15]. However, the above prescription will not affect the results in the temperature ranges relevant to the present study.

At large quark densities, the chiral symmetry restoring transition in PNJL model becomes first order. Figure 1 also shows the behavior of the chiral condensate and the Polyakov loop in the presence of a chemical potential $\mu_q = 320$ MeV, which is just above the critical point for this model. The transition temperature at this μ_q is ∼85 MeV. Note the sharp fall of $\langle \bar{u}u \rangle$, indicating a first-order transition. All the quantities shown in the figure show a jump at the transition point, consistent with a discontinuous transition, though the drop in $\langle \bar{s}s \rangle$ and the rise in Φ are only a few percent, and both these quantities have rather complicated temperature dependence above the transition point. In the presence of a chemical potential, there is no charge conjugation symmetry, so $\Phi \neq \bar{\Phi}$, as seen in Fig. 1(c).

One problem of the mean field study of PNJL model is the absence of color neutrality at finite density [16,17]. This arises because the Polyakov loop, which couples to the dynamical quarks, serves as an external colored field, leading effectively to separate chemical potentials for quarks of different color. As a remedy to this problem, it has been suggested to introduce a color chemical potential that will enforce color neutrality [16]. While this affects the individual number densities of the quarks of different colors, the total number densities of quarks and antiquarks, n_q and $n_{\bar{q}}$, do not change significantly [17]. We will discuss in Sec. IV B the implication of this for our study.

In Fig. 2, we show the variation of M_u and M_s with temperature at different chemical potentials. Here M_u and M_s are the constituent quark masses, Eq. (6). At $\mu_q = 0$, the change in the mass is smooth. But the change becomes sharper on introducing a chemical potential. While the introduction of the Polyakov loop changes the constituent quark masses considerably around the phase boundary, at very high temperature both models give similar results, since there $\Phi \to 1$. A similar variation of the strange quark mass is obtained in the two models.

The phase diagram we obtain is shown in Fig. 3. The critical point in our calculation was found to be at $(\mu_c, T_c) =$ (314 MeV, 92 MeV). While lattice estimates of the critical chemical potential μ_c vary considerably between different groups, they tend to be much lower than the PNJL value, $\leqslant$150 MeV. This probably indicates that the naive PNJL (or NJL) model may not be a good model for the QCD transition at large μ_q of ∼300 MeV, since nuclear excitations become important in this regime.

Another point to mention here is that the $U_A(1)$ anomaly term is introduced explicitly in the NJL and PNJL models by

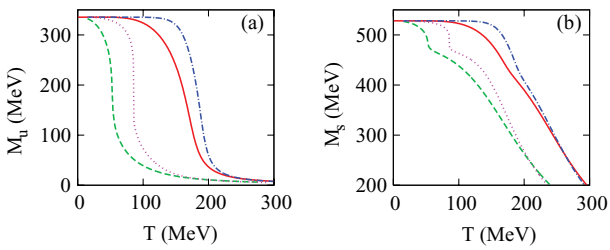

FIG. 2. (Color online) Variation of (a) M_u and (b) M_s with temperature, at $\mu = 0$ and 320 MeV for both NJL and PNJL models. Solid (red) and dashed (green) lines are for the NJL model with $\mu_q = 0$ and 320 MeV, respectively; dashed-dot (blue) lines and dotted (pink) lines show the corresponding figures for the PNJL model.

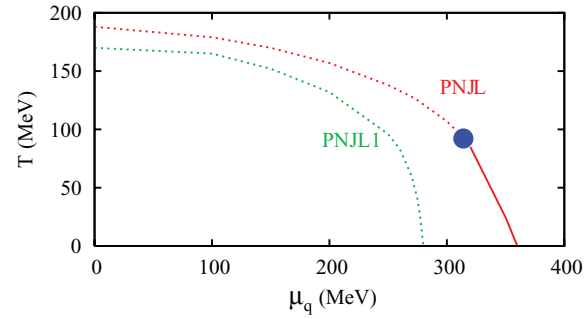

FIG. 3. (Color online) Phase diagram in the PNJL model. The solid line at large μ_q ends in a critical point at $(\mu_c, T_c) =$ (314 MeV, 92 MeV). At smaller μ_q, one gets a crossover, denoted by the dotted line. Inserting an explicit temperature dependence in the anomaly term $g_D(T) = g_D(0) \exp(-T/T_\chi)^2$ (denoted PNJL1; see text) washes off the first-order line completely.

a six-fermion interaction term. In QCD, of course, this term is introduced because of the instantons, which are topological objects in the gauge sector [18]. It is not known how well the anomalous $U_A(1)$ symmetry is restored in the deconfined phase. In Ref. [6] it was speculated that the $U_A(1)$ symmetry is restored well below T_χ. While there is no evidence of that from lattice studies, it is an open question whether the $U_A(1)$ symmetry is restored (or at least, the effect of the anomaly term substantially reduced) at above T_χ. If we include an explicit temperature dependence of the coefficient of the anomaly term, $g_D(T) = g_D(0) \exp[-T/T_\chi(\mu)]^2$, where $T_\chi(\mu)$ is the transition temperature at quark chemical potential μ, then the transition becomes considerably softer and the first-order line completely disappears, while the transition temperature moves to a somewhat lower value (see Fig. 3). We use PNJL1 to denote the model with such a temperature dependence of g_D in Eq. (2). One might be tempted to conclude that the existence of a critical point is strongly related to the strength of the instanton-induced anomaly term at the transition point.[2]

Of course, PNJL1 implies a substantial reduction of the anomaly term already before T_χ. A more realistic temperature dependence of g_D could be a sharp drop around T_χ. To investigate the effect of such a temperature dependence, we also consider Eq. (2) with $g_D(T) = g_D(0)\,(1 - \tanh 5x)/2$, where $x = (T - T_\chi(\mu))/T_\chi(\mu)$. We call this model PNJL2.[3] PNJL2 has a phase diagram similar to PNJL, i.e., the critical

[2]The effect of the anomaly term on the phase diagram has also been explored by Fukushima [11]. He used different values of g_D in Eq. (2) and found that for small g_D the first-order line disappears. In our analysis, the vacuum g_D is set from the η' mass and is not changed; but at finite temperature, we take $g_D(T) = g_D \exp(-T/T_\chi)^2$.

[3]This is essentially a smoothened version of a step jump at T_χ. The factor 5 is chosen arbitrarily so that $g_D(T)/g_D(0)$ is similar to PNJL1 at $1.05T_\chi$. Of course, a larger factor would have given a sharper drop. Note also that the $U_A(1)$ cutoff, in both PNJL1 and PNJL2, is a cutoff at both finite temperature and density, through the μ dependence of T_χ.

point has the same position at $(\mu_c, T_c) = (314\ \text{MeV}, 92\ \text{MeV})$. However, as we will see later, the nature of the mesonic excitations around T_χ can be substantially different between the two.

IV. MESONIC EXCITATIONS AND $U_A(1)$ ANOMALY

To understand the properties of the medium beyond the bulk thermodynamic properties, we need to look at the low-lying excitations. The simplest gauge invariant excitations in QCD are the mesonic excitations. Masses and decay widths of the mesonic resonances are calculated from the correlations of $\bar{q}\Gamma q$-type operators in QCD vacuum. In the medium, we are interested in spectral changes due to interactions with the medium; in particular, we would be interested in possible resonance-like structures in the deconfined phase. We need therefore to look at the spectral functions.

Here we study spectral functions of pseudoscalar and scalar mesonic states. They are of interest because of their close connection with the chiral-symmetry breaking and its restoration. The temperature dependence of the spectral function has been studied in the Nambu–Jona-Lasinio model in Ref. [6]. There it was found that narrow structures persist in the symmetry-restored phase, at moderately high temperatures. Here we intend to see how the coupling with the Polyakov loop affects these results. Also we study the sensitivity of these structures on the coefficients of the anomaly term. We also extend the studies to nonzero quark chemical potentials.

A. Formalism

The spectral function $\sigma_M(\omega, \mathbf{k})$ for a given mesonic channel M in a system at temperature T can be defined through the Fourier transform of the real-time two-point functions $D^>$ and $D^<$ [19],

$$\sigma_M(\omega, \mathbf{k}) = \frac{1}{2\pi}(D_M^>(k_0, \vec{k}) - D_M^>(k_0, \vec{k})), \tag{11}$$

$$D_M^{>(<)}(k_0, \vec{k}) = \int \frac{d^4x}{(2\pi)^4} e^{ik.x} D_M^{>(<)}(x_0, \vec{x}),$$

$$D_M^>(x_0, \vec{x}) = \langle J_M(x_0, \vec{x}) J_M(0, \vec{0})\rangle_c, \tag{12}$$

$$D_M^<(x_0, \vec{x}) = \langle J_M(0, \vec{0}) J_M(x_0, \vec{x})\rangle_c.$$

Here J_M is the suitable hadronic operator, and the subscript c denotes the connected part of the correlation function. Using the Kubo-Martin-Schwinger (KMS) condition [19]

$$D_M^>(x_0, \vec{x}) = D^<(x_0 + i/T, \vec{x}), \tag{13}$$

one can connect $\sigma_M(\omega, \mathbf{k})$ to the retarded correlation function,

$$\sigma_M(\omega, \mathbf{k}) = 2\pi \text{Im} D_M^R(k_0, \vec{k}),$$

$$D_M^R(k_0, \vec{k}) = \int \frac{d^4x}{(2\pi)^4} e^{ik.x} \theta(x_0) \langle [J_M(x_0, \vec{x}), J_M(0, \vec{0}]\rangle_c. \tag{14}$$

Inserting a complete set of states in Eq. (11) and using Eq. (13), one gets the expansion

$$\sigma_M(\omega, \mathbf{k}) = \frac{(2\pi)^2}{Z} \sum_{m,n} (e^{-E_n/T} \pm e^{-E_m/T}) \times |\langle n|J_M(0)|m\rangle|^2 \delta^4\left(k_\mu - q_\mu^n + q_\mu^m\right), \tag{15}$$

where Z is the partition function, and q^n refers to the four-momenta of the state $|n\rangle$.

A stable mesonic state contributes a δ function-like peak to the spectral function:

$$\sigma_M(\omega, \mathbf{k}) = |\langle 0|J_M|M\rangle|^2 \epsilon(k_0) \delta\left(k^2 - m_M^2\right), \tag{16}$$

where m_M is the mass of the state. For an unstable particle, one gets a peak with a finite width, e.g., the Breit-Wigner form for states with narrow decay width. We want to study how the spectral function changes as a result of collisions with the thermal medium.

At the level of approximation we are working, the collective excitations, that is, the fluctuation of the mean field around the vacuum, can be handled within the random-phase approximation (RPA) [20]. In this approximation, which is equivalent to summing over the ring diagrams, the retarded correlation function is given by

$$D_M^R = \frac{\Pi_M}{1 - 2G\Pi_M}. \tag{17}$$

Here G is the suitable coupling constant, and $\Pi_M(k^2)$ is the one-loop polarization function for the mesonic channel under consideration, i.e.,

$$\Pi_M(k^2) = \int \frac{d^4p}{(2\pi)^4} \text{Tr}\left[\Gamma_M S\left(p + \frac{k}{2}\right) \Gamma_M \left(p - \frac{k}{2}\right)\right]. \tag{18}$$

$S(p)$ is the quark propagator and Γ_M is the effective vertex factor. Equation (18) has been evaluated in the literature; for the NJL model, the effective formulas were calculated in Ref. [6]. The whole effect of the introduction of the background Polyakov loop can be absorbed into a modification of the Fermi-Dirac distribution functions [12]

$$f_\Phi^+(E_p) = \frac{(\bar{\Phi} + 2\Phi\, e^{-\beta(E_p+\mu)}) e^{-\beta(E_p+\mu)} + e^{-3\beta(E_p+\mu)}}{1 + 3(\bar{\Phi} + \Phi e^{-\beta(E_p+\mu)}) e^{-\beta(E_p+\mu)} + e^{-3\beta(E_p+\mu)}}, \tag{19}$$

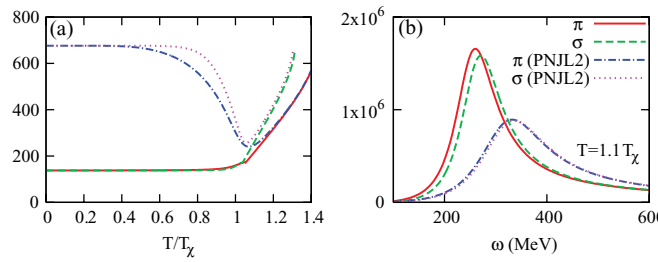

FIG. 4. (Color online) (a) Pion and σ mass vs temperature, at $\mu = 0$ MeV for the NJL (red, solid, and blue dash-dotted) and PNJL (green, dashed and pink, dotted) models. (b) Spectral functions for the pion and σ in the PNJL model, just above T_χ. Also shown is the effect of suppression of the anomaly term at T_χ (PNJL2; see Sec. III) on the spectral functions.

$$f_\Phi^-(E_p) = \frac{(\Phi + 2\bar{\Phi}\, e^{-\beta(E_p-\mu)})\, e^{-\beta(E_p-\mu)} + e^{-3\beta(E_p-\mu)}}{1 + 3(\Phi + \bar{\Phi} e^{-\beta(E_p-\mu)}) e^{-\beta(E_p-\mu)} + e^{-3\beta(E_p-\mu)}}. \tag{20}$$

For the NJL model, $\Phi = 1$ and the distribution functions become the usual Fermi-Dirac distribution function.

From the correlation function, one can calculate the spectral function using Eq. (14). The position of the pole controls the decay of the correlator and is called the pole mass. It can be obtained by solving

$$1 - 2G\Pi_M = 0. \tag{21}$$

The coupling constants G for the different flavor combinations are given in Table I. The cases of η and η' need a special mention. These mesons arise from the mixing of the flavor singlet and octet states, i.e., η_0 and η_8 mesons. The mixing arises because of an interplay between the anomaly term and the nondegeneracy between m_s and $m_{u,d}$. The masses of η and η' may be obtained from the roots of the equation

$$\det[1 - 2\Pi G] = \det \begin{pmatrix} 1 - (2\Pi_{00}G_{00} + 2\Pi_{80}G_{80}) & -(2\Pi_{00}G_{08} + 2\Pi_{08}G_{88}) \\ -(2\Pi_{00}G_{80} + 2\Pi_{88}G_{80}) & 1 - (2\Pi_{80}G_{08} + 2\Pi_{88}G_{88}) \end{pmatrix} = 0, \tag{22}$$

where

$$\begin{aligned} \Pi_{00} &= \frac{2}{3}\left[2\Pi^P_{uu}(k) + \Pi^P_{ss}(k)\right], \\ \Pi_{08} &= \left(\frac{2\sqrt{2}}{3}\right)\left[\Pi^P_{uu}(k) - \Pi^P_{ss}(k)\right], \\ \Pi_{88} &= \frac{2}{3}\left[\Pi^P_{uu}(k) + 2\Pi^P_{ss}(k)\right]. \end{aligned} \tag{23}$$

The polarization functions are obtained from Eq. (18). On the other hand, pole masses of η_0 and η_8 can be obtained directly from Π_{00}, Π_{88}, and Eq. (21).

B. Results at finite temperatures

The pion and σ channels provide the most interesting observables with mesonic states, since they are directly associated with the chiral symmetry. In the chiral-symmetry-restored phase, pion and σ should be degenerate. Below T_χ, on the other hand, pion is the Goldstone mode of the spontaneously broken chiral symmetry and is therefore much lighter than the σ.

In Fig. 4, we show the temperature dependence of the pole masses of the pion and the σ in the NJL and PNJL models. We see that close to T_χ there is substantial difference between the two models. While the two states come close to each other, they are not degenerate just above T_χ. As mentioned in Sec. III, results of the two models converge at higher temperatures. This, combined with the fact that T_χ is lower for the NJL model, leads to a smoother change in the NJL model above T_χ than in the PNJL. The nondegeneracy between the pion and the σ can also be seen in the Fig. 4(b), which shows the spectral functions in the pion and σ channels at a temperature of $1.1T_\chi$.

There can be two sources for the nondegeneracy: the finite (though small) current quark masses, and the remnant $U_A(1)$ symmetry. To investigate the effect of the $U_A(1)$ symmetry, we look at PNJL2, which introduces a cutoff in g_D, as explained in Sec. III. As can be seen in Fig. 4, this significantly alters the spectral functions, and removes most of the nondegeneracy of the π and σ above T_χ. Also, while there is a clear structure in both of these channels above T_χ, the structure is considerably broader in the absence of the anomaly term. When studying remnant bound state structures from QCD-inspired models, it therefore is important to keep in mind the effect of the anomaly term, since unlike in QCD, the anomaly terms are put in here by hand and therefore their contributions across phase transition may be different from that in QCD.

In Fig. 5, we have plotted the masses of η, η', η^0, and η^8 mesons. We see features similar to those in Fig. 4: significant differences around the transition region due to the introduction of the Polyakov loop. It is also seen that very close to the transition region, the masses of the singlet and octet states start approaching each other, indicating that the effect of the anomaly term starts getting reduced. However, without an explicit cutoff as in PNJL2, the nondegeneracy between these two states is clearly visible at $1.1T_\chi$.

TABLE I. Pseudoscalar coupling strengths in the SU(3) NJL model, where $\alpha = \langle\bar{u}u\rangle$, $\beta = \langle\bar{d}d\rangle$, and $\gamma = \langle\bar{s}s\rangle$ [5,6].

$G_\pi = g_S + g_D\gamma$	$G_{K^\pm} = g_S + g_D\beta$
$G_{K^0} = g_S + g_D\alpha$	$G^P_{00} = g_S - \frac{2}{3}(\alpha + \beta + \gamma)g_D$
$G^P_{33} = G_\pi$	$G^P_{88} = g_S - \frac{1}{3}(\gamma - 2\alpha - 2\beta)g_D$
$G^P_{03} = -\frac{1}{\sqrt{6}}(\alpha - \beta)g_D$	$G^P_{38} = \frac{1}{\sqrt{3}}(\alpha - \beta)g_D$
$G^P_{08} = -\frac{\sqrt{2}}{6}(2\gamma - \alpha - \beta)g_D$	

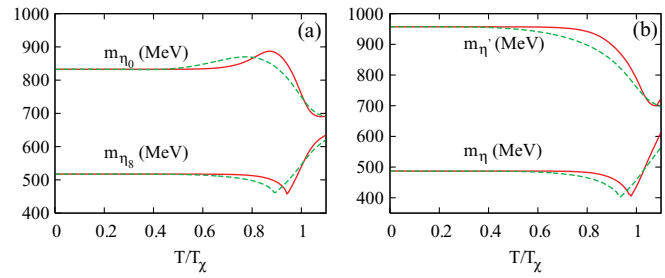

FIG. 5. (Color online) Masses of the different η states in NJL (green, dashed) and PNJL (red, solid) models.

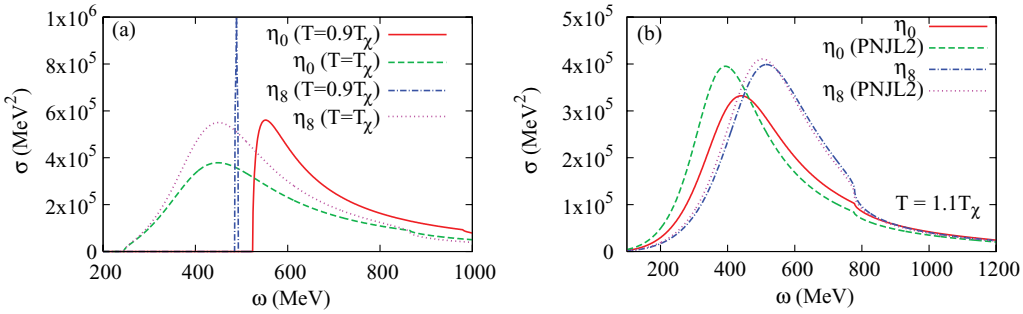

FIG. 6. (Color online) Spectral functions of $\eta_{0,8}$. (a) At temperatures of $0.9T_\chi$ and T_χ; note the δ function peak for η_8 below T_χ. (b) At temperatures above T_χ. Also shown are the effects of cutting off the anomaly term above T_χ at T_χ (PNJL2; see Sec. III).

The spectral functions of the η_0 and η_8 states, calculated in the PNJL model, are shown in Fig. 6. Here we also investigate the effect of the anomaly term by comparing the calculations in the PNJL2 model. We find here that the effect of the anomaly term is considerable in η_0 but not in η_8. This can be understood by looking at the two relevant couplings, G_{88} and G_{00}, in Table I. Because of the different numerical factors and the different combinations of the quark condensates, the anomalous coupling of η_0 is substantially larger than that of η_8. Interestingly, the broadening due to anomaly suppression is much less even for η_0 than was seen for the pion. In these channels, a clear (though broad) resonance structure is seen just above T_χ.

The behavior of the pole mass for the kaon state (Fig. 7) is qualitatively similar to the pion. However, the spectral function above T_χ, shown in the same figure, shows a very different behavior. The sharp peak at T_χ is completely washed off already by $1.1T_\chi$: there is no indication of a strong correlation between quarks in this channel.

C. Results at finite densities

One of the advantages of model studies is that one can study regions in parameter space that are not easy to study directly from QCD in a controlled way. The agreement of PNJL model results with QCD at finite temperatures encourages us to investigate effects of nonzero baryon densities, by introducing a quark chemical potential. As mentioned in Sec. III, however, we do not expect the PNJL model to be a good model for QCD transition at large μ_q. We therefore investigate the mesonic excitations in this model at $\mu_q = 150$ MeV. This is around the region where lattice studies suggest the beginning of the first-order line, while the PNJL model still finds a crossover transition at these densities. From Fig. 3, we also get $T_\chi \sim 170$ MeV at $\mu_q = 150$ MeV, which is not too far from what one gets from lattice.

In Fig. 8, we show the pion and σ spectral functions above T_χ for $\mu_q = 150$ MeV. We see that the spectral functions have a sharp structure even substantially above T_χ, as in the case for $\mu_q = 0$. The nondegeneracy of the two channels and the effect of the anomaly terms are also similar to the $\mu_q = 0$ case. In the Figs. 8(b) and 8(c) we show the variation of the pion pole mass with μ_q, for two different temperatures. Interestingly, the quantitative difference in the masses calculated in PNJL and NJL models increases with density. Of course, as we have discussed above, we do not expect these models to be a good approximation to QCD at values of $\mu_q \gg 150$ MeV.

The spectral functions of η_0 and η_8 are shown in Fig. 9, for $\mu_q = 150$ MeV. This figure has some interesting features. First, the interplay of the temperature and chemical potential gives rise to a nonmonotonous behavior in the peak of the η_8 spectral function in the deconfined phase. The peak position drops sharply at T_χ, and then rises again. Second, we note that the η_8 peak, which is below the η_0 peak below or at T_χ, becomes very broad already at $1.05T_\chi$, with the peak position slightly above that of the η_0 peak. If this feature is true for full QCD and is not an artefact of the model, it will have interesting phenomenological implications.

Let us now discuss the sensitivity of our results on enforcement of color neutrality (Sec. III). Our calculations

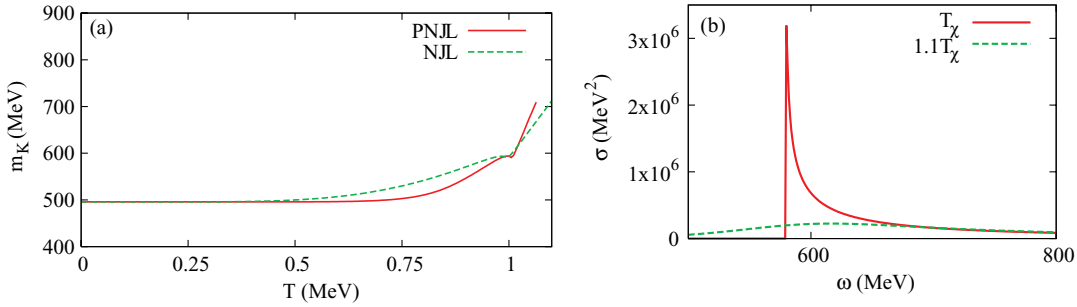

FIG. 7. (Color online) (a) Pole mass of the kaon state, in PNJL and NJL models, at different temperatures. (b) Spectral function, from the PNJL model. The sharp peak at T_χ seems to be completely washed off already by $1.1T_\chi$.

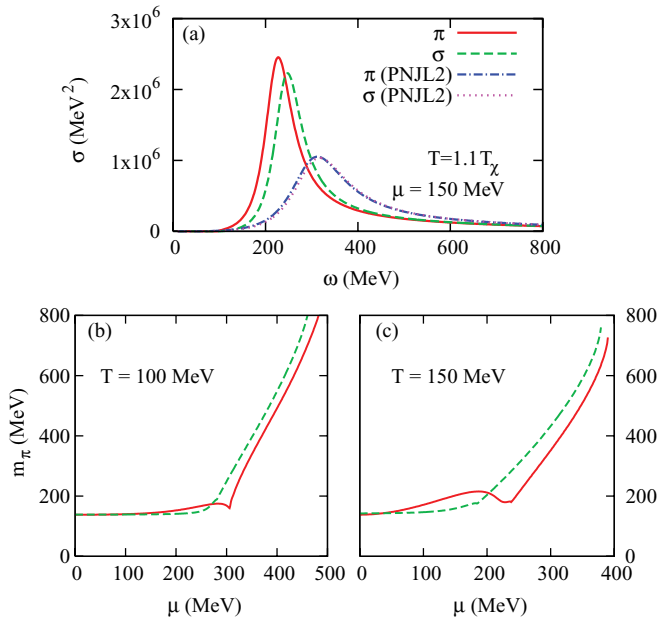

FIG. 8. (Color online) (a) Spectral functions of pion near the chiral transition point, for $\mu_q = 150$ MeV. Also shown is the effect of suppression of the anomaly term at T_χ (PNJL2; see Sec. III). (b) Pion mass vs μ, at $T = 100$ MeV. Solid red line is for PNJL model and dashed green line is for NJL model. (c) Same as (b), but at $T = 150$ MeV.

at finite density have been carried out at $\mu = 150$ MeV and $T = 1.1T_c$. At such T and μ, if we want to enforce color neutrality by introducing a color chemical potential, we need a color chemical potential $\mu_3 T_3 + \mu_8 T_8$ (in the notation of Ref. [16]) with a small μ_8 (∼30 MeV), while μ_3 is negligible. Here T_3 and T_8 are Gell-Mann matrices in color space. While this changes the individual color densities, the total quark number density $(n_q - n_{\bar{q}})$ and the total scalar density $(n_q + n_{\bar{q}})$ do not have any appreciable change. Similar results about the total quark density have been reported in Ref. [17]. In fact, the change in the scalar density is less than 5% under such conditions. Here we have studied spectral functions of colorless, meson-like objects, which are sensitive to the scalar density. Hence we do not expect our results at finite chemical potential to be affected appreciably by the issue of color neutrality.

V. CONCLUSION

To conclude, we have studied the meson-like excitations in the deconfined plasma at both zero and nonzero quark chemical potential, using the Polyakov loop extended Nambu–Jona-Lasinio (PNJL) model.

The phase diagram of the PNJL model shows a first-order line of transitions at large μ_q, ending in a critical point at $(\mu_c, T_c) \sim (314\ \text{MeV}, 92\ \text{MeV})$. We note, however, that the phase diagram can be quite sensitive to the temperature dependence of the coefficient of the anomaly term. In particular, a suppression of the anomaly term at large temperatures may lead to a complete wash off of the first-order line.

The in-medium behavior of the mesonic correlations was studied by looking at the spectral functions. In the pion and σ channels, a reasonably sharp structure was found still at $1.1T_\chi$; also the two states are not degenerate at these temperatures. While both these features can be phenomenologically interesting, it was also found that these features are quite sensitive to the anomaly term. In particular, suppressing the anomaly term above T_χ leads to much broader and degenerate structures in these two channels. Since the structure of the π resonance above T_χ is of importance for RHIC phenomenology, this sensitivity implores one to look for the restoration or otherwise of the $U(A)_1$ anomaly at T_χ by looking at suitable observables directly on lattice.

The η_8 and the η_0, on the other hand, show much less sensitivity to the anomaly term. Both these channels show a clear resonance at $1.1T_\chi$. η_8 shows very little sensitivity to a suppression of the anomaly term. η_0 is more sensitive, but the resonance-like structure remains even when the anomaly term is suppressed. In the PNJL model, the kaon channel does not show any sharp structure above T_χ. All these behaviors will be of interest for RHIC phenomenology.

We also looked at the mesonic spectral functions just above T_χ for a nonzero μ_q. At $\mu_q = 150$ MeV, which should be in the regime covered by the RHIC energy scan, PNJL shows a crossover transition. The features of the spectral functions

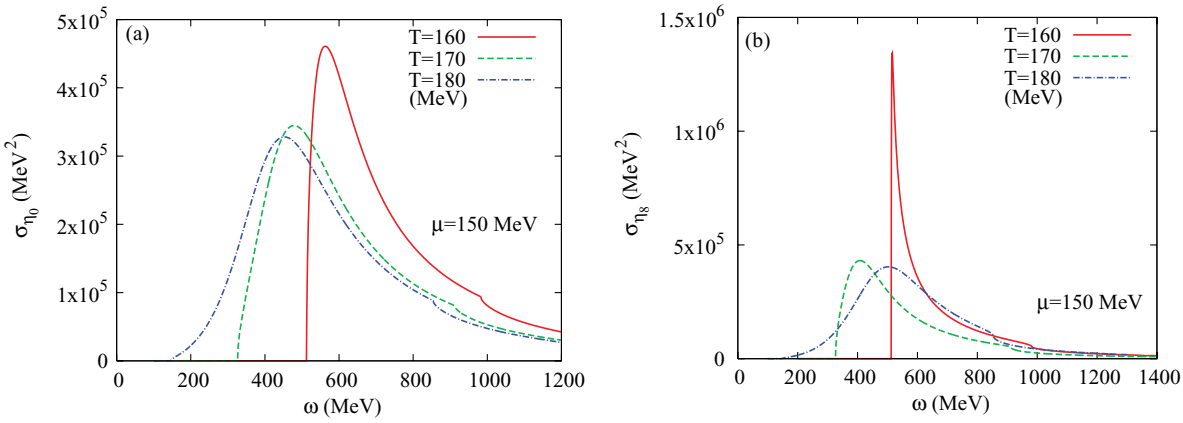

FIG. 9. (Color online) Spectral functions of the (a) η_0 and (b) η_8 channels around the chiral transition temperatures, for $\mu_q = 150$ MeV.

in the pion and σ channels are found to be quite similar to those at $\mu_q = 0$. A more interesting behavior was found in the η channels. The interplay of the finite μ_q and finite T lead to a nonmonotonous behavior of the peak in the η_8 channel. Also it was found that the relative positions of the η_0 and η_8 peaks become reversed above T_χ: the η_0 peak comes at a lower ω than the η_8 peak at $1.05T_\chi$. It will be interesting to explore the phenomenological implications of these behaviors.

ACKNOWLEDGMENTS

P.D. thanks Council of Scientific and Industrial Research (CSIR) for financial support. A.B. thanks CSIR for support through the Project No. 03(1074)/06/EMR-II and acknowledges a University Grants Commission and University for Potential Excellence grant (computational support). SKG thanks Department of Science and Technology, Govt. of India, for financial support under the IRHPA scheme.

[1] Z. Fodor and S. D. Katz, J. High Energy Phys. 04 (2004) 050; C. R. Allton *et al.*, Phys. Rev. D **68**, 014507 (2003); R. V. Gavai and S. Gupta, Phys. Rev. D **78**, 114503 (2008).
[2] P. de Forcrand and O. Philipsen, Nucl. Phys. **B673**, 170 (2003).
[3] M. Cheng *et al.*, Phys. Rev. D **74**, 054507 (2006).
[4] Y. Aoki, G. Endrodi, Z. Fodor, S. D. Katz, and K. K. Szabo, Nature (London) **443**, 675 (2006).
[5] S. P. Klevansky, Rev. Mod. Phys. **64**, 649 (1992).
[6] T. Hatsuda and T. Kunihiro, Phys. Rep. **247**, 221 (1994).
[7] K. Fukushima, Phys. Lett. **B591**, 277 (2004).
[8] C. Ratti, M. A. Thaler, and W. Weise, Phys. Rev. D **73**, 014019 (2006).
[9] S. K. Ghosh, T. K. Mukherjee, M. G. Mustafa, and R. Ray, Phys. Rev. D **73**, 114007 (2006).
[10] S. Mukherjee, M. G. Mustafa, and R. Ray, Phys. Rev. D **75**, 094015 (2007).
[11] K. Fukushima, Phys. Rev. D **77**, 114028 (2008).
[12] H. Hansen, W. M. Alberico, A. Beraudo, A. Molinari, M. Nardi, and C. Ratti, Phys. Rev. D **75**, 065004 (2007).
[13] P. Costa, M. C. Ruivo, C. A. de Sousa, H. Hansen, and W. M. Alberico, arXiv:0807.2134.
[14] M. Ciminale, R. Gatto, N. D. Ippolito, G. Nardulli, and M. Ruggieri, Phys. Rev. D **77**, 054023 (2008).
[15] S. K. Ghosh, T. K. Mukherjee, M. G. Mustafa, and R. Ray, Phys. Rev. D **77**, 094024 (2008).
[16] H. Abuki, M. Ciminale, R. Gatto, G. Nardulli, and M. Ruggieri, Phys. Rev. D **77**, 074018 (2008); H. Abuki, M. Ciminale, R. Gatto, and M. Ruggieri, Phys. Rev. D **79**, 034021 (2009).
[17] H. Abuki and K. Fukushima, arXiv:0901.4821.
[18] G. 't Hooft, Phys. Rev. Lett. **37**, 8 (1976).
[19] M. LeBellac, *Thermal Field Theory* (Cambridge University, New York, 1996).
[20] A. L. Fetter and J. D. Walecka, *Quantum Theory of Many-Particle System* (McGraw-Hill, New York, 1971).